Quantum Properties of Low-Dimensional Antiferromagnets

Proceedings of French-Japanese Symposium

Held in Fukuoka, Japan
November 20-22, 2001

Under the Auspices of Japan Society for the Promotion of Science (JSPS),
Centre National de la Recherche Scientifique, France (CNRS),
and Kyushu University

Edited by
Yoshitami Ajiro
Jean-Paul Boucher

Kyushu University Press

Spin frustration in two-dimensional compounds: $SrCu_2(BO_3)_2$, γ-$Cu_2(OH)_3Cl$, $Cu_2(OH)_3Br$

H. Kageyama, T. Nakajima, M. Ichihara, F. Sakai and Y. Ueda

Material Design and Characterization Laboratory, The Institute for Solid State Physics, The University of Tokyo, Kashiwanoha 5-1-5, Kashiwa, Chiba 277-8581, Japan

Structural and magnetic properties of two-dimensional spin-1/2 frustrated systems are presented. The structure of $SrCu_2(BO_3)_2$ comprises of a combination of Shastry-Sutherland and Gelfand models. We find that Ba- and Ca-replacement for the Sr site modifies the interlayer distance, leading to a systematic change in the structural transition temperature. γ-$Cu_2(OH)_3Cl$ containing an ideal Kagomé lattice possibly undergoes a weak ferromagnetic transition at 7 K, while a distorted triangular system $Cu_2(OH)_3Br$ exhibits a complex behavior at low temperatures.

PACS number: 75.40.Cx, 75.50.Ee

1. INTRODUCTION

Problem of spin frustration in general arises either from (1) a disorder effect in solid solutions with different types of exchange interaction (ferromagnetic/antiferromagnetic) and/or anisotropy (Ising/XY/Heisenberg), or from (2) a particular structure that does not allow antiferromagnetically coupled spins to find any ordinary way of ordering in the lattice. The latter has been a subject of intensive research because special geometry -triangular lattice and Kagomé lattice to name only a few- gives rise to novel ground states, sometimes accompanied by sequential phase transitions as a function of temperature T or magnetic field H.

In this paper, we will treat following three cuprates that can be viewed as two-dimensional (2d) spin-1/2 frustrated systems: $SrCu_2(BO_3)_2$, γ-$Cu_2(OH)_3Cl$ and $Cu_2(OH)_3Br$. The borate is the orthogonal dimer system with an exact dimer ground state [1, 2]. The chloride may be a good candidate for an S=1/2 Heisenberg Kagomé lattice with no lattice distortion, while the bromide, isostructural with α-$Cu_2(OH)_3Cl$, has a triangular-like lattice. We shall argue the magnetic properties of these materials putting a special emphasis on the relation to each geometry.

2. EXPERIMENTAL

The powder samples of the solid solution $Sr_{1-x}A_xCu_2(BO_3)_2$ (A=Ca, Ba; $0<x<0.3$) were obtained by firing in air at 800-900 °C (dependant on the nominal composition) a mixture of a stoichiometric starting reagents $SrCO_3$, ACO_3, CuO, along with 5 % molar excess of B_2O_3 to compensate for the loss due to volatilization. The lattice parameters as a function of T and x were determined by powder X-ray diffraction technique using a M21X diffractometer (Mac Science) with CuK_α radiation. The microscopic structure of $SrCu_2(BO_3)_2$ was analyzed by means of transmission electron microscope (TEM) using JEM2010F (JOEL).

There are some isomorphs of $Cu_2(OH)_3Cl$, e.g., α-, β-, and γ-forms with the space groups *Pnam* (orthorhombic), *P*2*1*/*m* (monoclinic) and *R*-3*mH* (trigonal), respectively [3]. The γ-type of interest was selectively obtained by boiling 100 cc of 0.25 M-$CuCl_2$ with 1.5 g of Cu fine powder flowing oxygen gas for a couple of days. $Cu_2(OH)_3Br$ was synthesized by a hydrothermal reaction at 300 °C using an autoclave with 0.25 g of CuO in 15 cc of 2 M-$CuBr_2$ [4]. Magnetic properties were conducted using a MPMS magnetometer (Quantum Design).

3. ORTHOGONAL DIMER LATTICE

3.1 Crystal structure

Let us begin with the 2d copper dimer network in $SrCu_2(BO_3)_2$ viewed along the [001] direc-

tion (Fig.1(a)), which is topologically equivalent to the Shastry and Sutherland model [1], where J and J' denote, respectively, the intra- and interdimer exchange constants. The orthogonal arrangement of nearest-neighbor dimer pairs gives rise to the exactly solvable ground state [1, 2] as well as extremely localized triplet excitations [5, 6]. As shown in Fig. 2, the TEM reflections and the image both taken along [001] at R.T. is in good accordance with the tetragonal symmetry (I-42m) [7] and also ensures high quality of the sample.

Although the magnetism of $SrCu_2(BO_3)_2$ can be mostly described by the 2d Shastry-Sutherland theory, the necessity of introducing three dimensionality into account has been recently claimed [8, 9] along with a generalized 3d phase diagram [10]. Displayed in Fig. 1(b) is the dimer arrangement along the c axis, topologically equivalent to the model considered by Gelfand [11]. This ladder-like lattice with J and J'' (J'' : interlayer coupling) again satisfies the orthogonality, hence making its ground state exactly solvable and triplet excitations impossible to propagate. Now the physics of the similar kind is applicable for the real-life structure of $SrCu_2(BO_3)_2$ (Fig. 1(c)) since the 3d lattice is the very combination of Figs. 1(a) and 1(b) [12].

To be strict, the dimers in Fig. 1(a) do not sit on the same plane: as a result of a corrugation of the $CuBO_3$ layer, the plane of horizontal dimers is slightly shifted from that of vertical dimers along the ladder by 0.0445 Å at R.T. [7]. This buckling complicates the situation as follows. At first, a D vector for the Dzyaloshinski-Moriya (DM) interaction otherwise oriented along the c-axis tilts to some extent, causing (unfortunately or fortunately) rather complex dispersions of triplet excitations [14] and anomalous phonon modes [15]. At second, the otherwise uniform interdimer distance shrinks or elongates, thus making J'' alternated along the ladder.

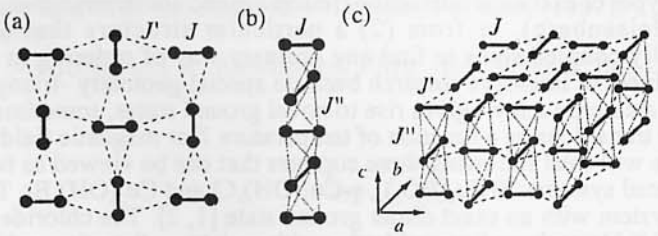

Fig. 1: (a) The 2d orthogonal Cu-dimers in $SrCu_2(BO_3)_2$ topologically equivalent to the Shasty-Sutherland model. (b) The 1d orthogonal Cu-dimers in $SrCu_2(BO_3)_2$ topologically equivalent to the Gelfand model. (c) The real 3d structure of $SrCu_2(BO_3)_2$.

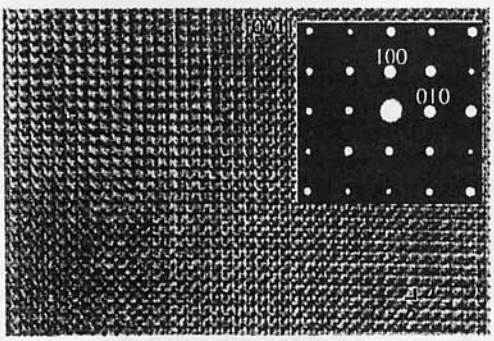

Fig. 2: The [001] TEM image and reflections of $SrCu_2(BO_3)_2$ at R.T.

3.2 Structural phase transition

Sparta et al. recently observed a 2nd-order structural phase transition at T_s=395 K, with the space group changing from I-42m to $I3/mcm$ [15]. Interestingly, the otherwise buckled $CuBO_3$ layer becomes completely flat above T_s. This finding has motivated us to examine the chemical pressure effect on the structural and magnetic properties, since, if the high-T phase is stabilized down to 0 K, one can treat a simpler magnetic system with a uniform J'' and without a tilt of D

with respect to the c axis.

Under the present synthetic condition, however, we were only able to obtain a partial solid solution $Sr_{1-x}A_xCu_2(BO_3)_2$ (A=Ca, Ba; $0<x<0.3$). Figure 3 compares the powder X-ray diffraction patterns for a 20 % Ca substituted sample between 573 K and 291 K, and the $\theta/2\theta$ scans around the (011) index taken at in-between temperatures are represented in Fig. 4. Just like the mother compound (x=0) [15], we have successfully observed the structural transition characterized by the following extinction rule for the high-T phase: ($0kl$) with $k+l$=odd. The temperature dependence of the (011) intensity for the solid solution, normalized by the intensities at R.T. (Fig. 5), allows us to estimate T_s. No discontinuous change suggests every transition to be also of a 2nd order transition. The values of T_s are determined as 365 K, 382 K, 401 K and 407 K for (Ca; x=0.2), (Ca; x=0.1), (Ba; x=0.1) and (Ba; x=0.2), respectively (see Fig. 6).

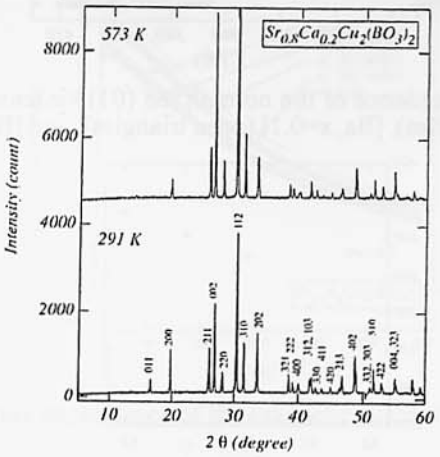

Fig. 3: The powder X-ray diffraction patterns of the 20 % Ca substituted $SrCu_2(BO_3)_2$ scanned at 573 K (upper) and 291 K (lower).

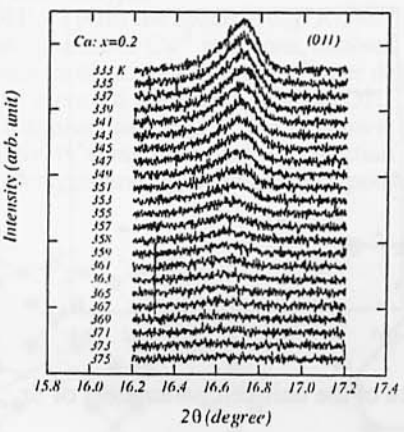

Fig. 4: The temperature variation of the (011) peak for the 20 % Ca substituted $SrCu_2(BO_3)_2$.

In Fig. 7, the lattice parameters at R.T. are plotted against x in $Sr_{1-x}A_xCu_2(BO_3)_2$. The shrink (expansion) of the a and c axes on replacing Ca (Ba) is consistent with the difference in the ionic radii which vary as $Ca^{2+}<Sr^{2+}<Ba^{2+}$. It is noted that the substitution effect appears much more significantly on the c parameter, reflecting the structural aspects featured by the rigid $CuBO_3$ planes with the Sr^{2+} ions embedded in between. We infer from these facts that T_s depends mainly on the interlayer distance. If so, further shrink of interlayer distance must lead to further lower-

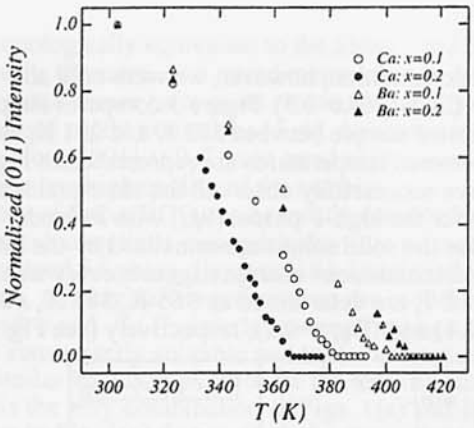

Fig. 5: The temperature dependence of the normalized (011) intensity for [Ca, x=0.2] (solid circles), [Ca, x=0.1] (open circles), [Ba, x=0.1] (open triangles), and [Ba, x=0.2] (solid triangles).

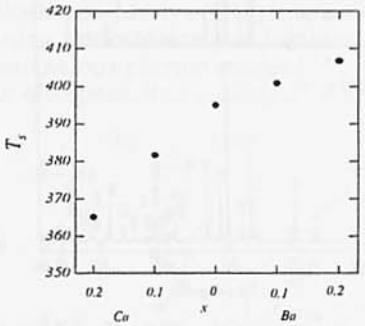

Fig. 6: The structural transition temperature T_s plotted against x in $Sr_{1-x}A_xCu_2(BO_3)_2$.

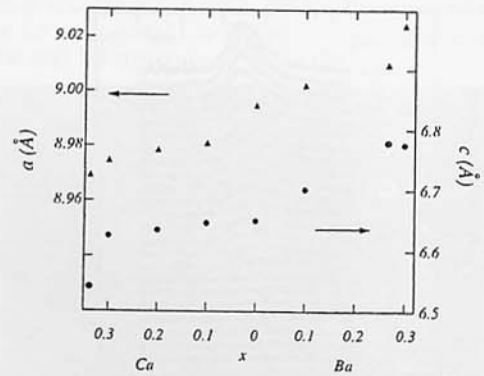

Fig. 7: Composition dependence of the unit-cell parameters of $Sr_{1-x}A_xCu_2(BO_3)_2$ (A: Ca or Ba) obtained at R.T.

ing of T_s. However, a glance at Fig. 6 naively suggests that T_s would be at most 250 K even if one could achieve the Ca-end, i.e., $CaCu_2(BO_3)_2$.

Apart from the structural transition, it is a matter of interest to see the influence of magnetic properties. We show in Fig. 8 magnetic susceptibility vs. temperature plotting for $Sr_{1-x}A_xCu_2(BO_3)_2$. We practically encounter a difficulty in determining the exchange constants upon doping because our data in high-T region are somewhat scattered, exhibiting no systematic change as a

function of x. This may be related to inhomogeneity of the samples, a problem inevitably involved in solid solutions. Nevertheless, one clearly notices that the susceptibilities for all the samples including x=0 take maxima at the same temperature 16 K and then drops toward zero as $T \rightarrow 0$. Apparently, the spin gapped ground state is unchanged on the substitution at least up to 30 %. That is to say, the set of exchange interactions (J, J' and J'') is not yet enough to exceed the critical points to an antiferromagnetic or to a plaquette spin-singlet states as theoretical shown by the 3d phase diagram [10], although the theory does not assume the fact that J'' is, in reality, alternated along the ladder below T_s [7]. It should be mentioned that a hydrostatic pressure up to 10 kbar has failed to induce such transitions as well, but the temperature at maximum susceptibility tends to decreases slowly as the pressure rises [16].

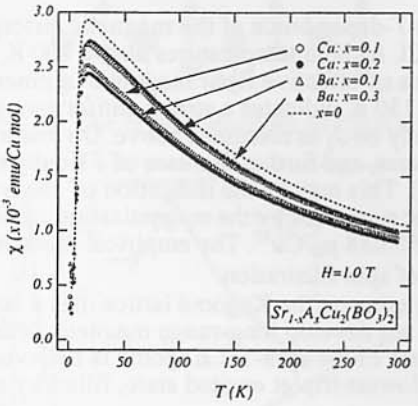

Fig. 8: The temperature dependence of the magnetic susceptibility of $Sr_{1-x}A_xCu_2(BO_3)_2$.

4. KAGOM´E LATTICE

4.1 Crystal Structure of γ-$Cu_2(OH)_3Cl$

The structure of γ-$Cu_2(OH)_3Cl$ with the space group R-3mH is displayed in Fig. 9 [3]. It has crystallographically two distinguishable Cu^{2+} positions, denoted as Cu(I) and Cu(II). The former builts a dilute triangular lattice in the *ab* plane, and the latter does a dense ideal Kagomé lattice, in contrast to the previously reported material $Cu_3V_2O_7(OH)_22H_2O$ with isosceles triangular units, namely, a distorted Kagomé lattice [17]. As is shown in Fig. 9(b), the triangular and Kagomé planes stack alternatively along the trigonal c direction. The $Cu(II)^{2+}$ ion is octahedrally surrounded by four planer oxygens and by two chlorines pointing opposite direction, to com-

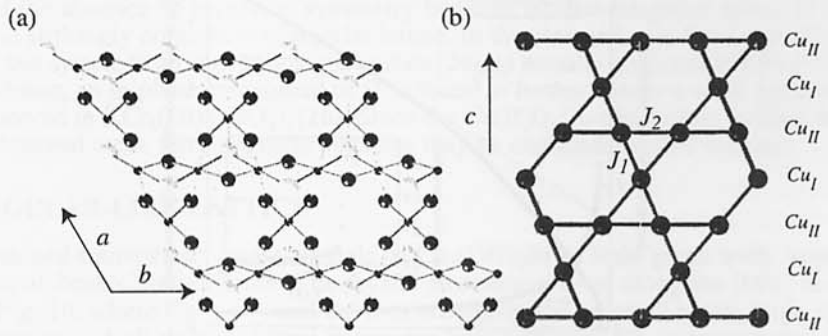

Fig. 9: The crystal structure of γ-$Cu_2(OH)_3Cl$. (a) $Cu(I)O_4Cl_2$ octahedra to give a Kagomé lattice. Cu(II) (black), O (gray) and Cl (white). (b) Cross-sectional veiw of a dense Kagomé and a dilute triangular lattices along the c axis.

plete a $Cu(II)O_4Cl_2$ pseudo octahedron (Fig. 9(a)), whereas the $Cu(I)^{2+}$ ion is centered in an oxygen-only octahedron. The neighboring $Cu(II)O_4Cl_2$ octahedra are coupled to edge-share, providing uniform superexchange (J_2) pathways in the Kagomé lattice. A shorter Cu(I)-Cu(II) distance (=3.059 Å) than that of Cu(I)-Cu(I) (=3.414 Å) does not lead to the conclusion that the interlayer interaction J_1 is larger than J_2 since a superexchange interaction in general is much more sensitive to the oxygen bridging angle. ∠Cu(I)-O-Cu(II) =96.9° responsible for J_1 is quite close to the critical angle of 97.6°, at which the exchange constant changes its sign [18]. On the contrary, J_2 is expected to be strongly antiferromagnetic judging from the corresponding oxygen bridging angle ∠Cu(II)-O-Cu(II) =119.0 °.

4.2 Magnetic Properties

In Fig. 10, we display the T-dependence of the magnetic susceptibility and the reciprocal susceptibility for γ-$Cu_2(OH)_3Cl$. At high temperatures above 100 K, the susceptibility well follows the Curie-Weiss law with an effective Bohr magnetic moment P_{eff} of 1.728 μ_B. The obtained Weiss constant θ_W = - 130 K indicates a strong antiferromagnetic spin-spin correlation which should be imposed mainly on J_2 as discussed above. On lowering T, however, a deviation from the Curie-Weiss law appears, and further decrease of T finally results in a steep increase in susceptibility below 7 K (=T_c). This may be the indication of the transition onto a weak ferromagnetic state, which is further supported by the magnetization curve at 5 K (not shown) with a spontaneous magnetization of 0.038 μ_B/Cu^{2+}. The empirical measure of frustration $f = -\theta_W/T_c$ is19, implying a large degree of spin frustration.

Theoretically, Heisenberg spins on the Kagomé lattice has a large number of degenerated ground states and hence does not develop long-range magnetic order at any temperatures [19, 20]. Especially, the ground state of the spin-1/2 Kagomé is believed to be spin-gapped with a finite excitation gap Δ to the lowest triplet excited state, filled by nonmagnetic excitations in between [21, 22, 23].

Seemingly, our experimental data contradict the theories on the spin-1/2 Kagomé. Still, a careful comparison allows us to find several interesting and hopeful features. According to Ref. [23], the theoretical susceptibility is strongly reinforced just above the spin gap. This effect may be related to the observed steep jump at 7 K and also the ferromagnetic deviation from Curie-Weiss law. Moreover, Waldtmann et al. claimed that Δ should be of the order of 0.025J [22, 23]. Considering the big reduction of Δ, the examination of a lower-temperature part (below 5 K) is needed in order to confirm the real ground state.

Although the present material possesses the ideal spin-1/2 Kagomé system, by which we mean there is no structural distortion, the system may require a correction coming from the residual exchange interaction J_1. In fact, the presence of the $Cu(I)^{2+}$ ions disables us to precisely

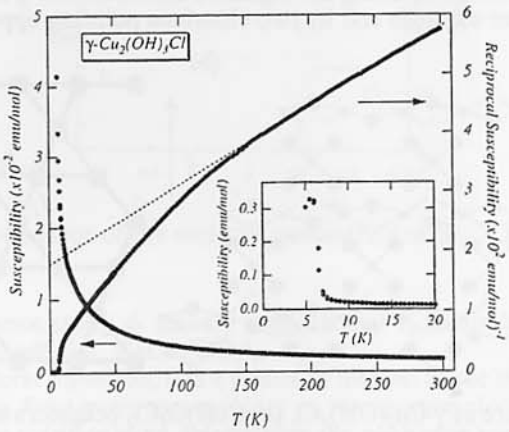

Fig. 10: The temperature variation of the magnetic susceptibility and reciprocal susceptibility for γ-$Cu_2(OH)_3Cl$. Enlarged plot below 20 K is shown in the inset.

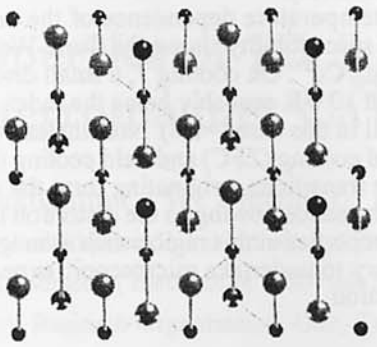

Fig. 11: The crystal structure of $Cu_2(OH)_3Br$.

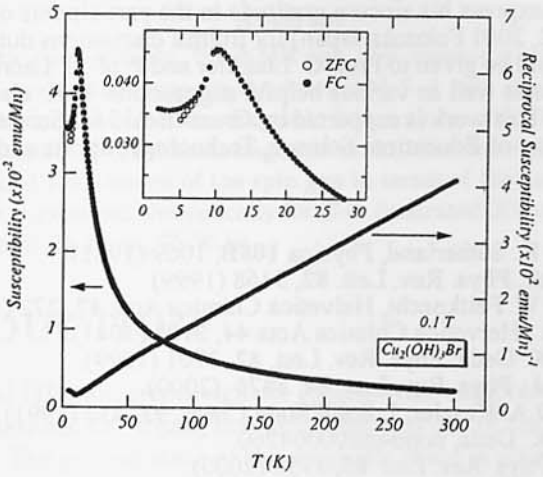

Fig. 12: The temperature variation of the magnetic susceptibility and reciprocal susceptibility for $Cu_2(OH)_3Br$.

estimate J_2 from the susceptibility data. Another candidate of perturbations is a DM interaction. Because of the absence of inversion symmetry between nearest-neighbor spins, D is always non-zero, in strikingly contrast to triangular lattice. In the classical spin limit, the DM interaction drives this system to an antiferromagnetic state [24], as actually observed in $KFe_3(OH)_6(SO_4)_2$ [25]. In addition, an in-plane component of D is found to further induce a weak ferromagnetism [24] as observed in $KCr_3(OH)_6(SO_4)_2$ [26]. Since the $Cu(II)O_4Cl_2$ octahedron is tilted from the c axis, the observed weak ferromagnetic behavior may be explained by this scenario.

5. TRIANGULAR-LIKE LATTICE

We obtained transparent single crystals of $Cu_2(OH)_3Br$ in light green with approximate dimensions of 2mm×2mm×0.1mm. The crystal structure viewed along the [001] direction is shown in Fig. 10, where Cu^{2+}, O^{2-}, and Br^- ions are expressed by small black, large black, and grey, respectively. A slightly distorted triangular lattice of spin-1/2 is constructed from two crystallographically inequivalent Cu^{2+} ions, one in a $Cu(I)O_4Br_2$ octahedron, and the other in a $Cu(II)O_5Br$ octahedron. Each $Cu(I)O_4Br_2$ unit edge-shares with two neighboring $Cu(I)O_4Br_2$ units and four neighboring $Cu(II)O_5Br$ units by sharing their edges, and vice versa. The in-plane

distances between neighboring coppers, Cu(I)-Cu(I), Cu(I)-Cu(II) and Cu(II)-Cu(II), are 3.069 Å, 3.231 Å and 3.070 Å, respectively.

In Fig. 11, we show the temperature dependence of the molar susceptibility and inverse susceptibility at H=0.1 T. The susceptibility shows the Curie-Weiss behavior down to 30 K, with θ_W= - 18.3 K and P_{eff} =1.733 μ_B/Cu^{2+}. On cooling T, a small discrepancy from Curie-Weiss law emerges, followed by a cusp at 10.0 K probably being the index of antiferromagnetic transition. The frustration factor f is small in this case (=1.8). Nonetheless, as shown in the inset of Fig. 11, a difference between zero field cooling (ZFC) and field cooling (FC) eventually appear at 7.5 K. This may be successful phase transitions, originating form the geometric frustration, although the frustration should be much reduced owing to the distortion in the lattice. To further characterize the peculiar magnetic properties in this region such as magnetic structure(s) and the origin of the hysteresis, it is necessary to undertake microscopic experiments, e.g., nuclear magnetic resonance and neutron diffraction.

ACKNOWLEDGMENTS

H.K. would like to express his sincere gratitude to the participants of French and Japanese symposium (Nov. 19-22, 2001 Fukuoka Japan) for fruitful discussions during and after the meeting. Special thanks should be given to Prof. C. Lhuillier and Prof. C. Lacroix for kindly showing their preliminary results as well as various helpful suggestions. H.K. also appreciates Cope K. for fruitful discussions. This work is supported by Grant-in-Aid for Scientific Research (C) (No. 40302640) from Ministry of Education, Science, Technology, Sports and Culture, Japan.

REFERENCES

1. B. S. Shastry and B. Sutherland, Physica **108B**, 1069 (1981).
2. H. Kageyama et al., Phys. Rev. Lett. **82**, 3168 (1999).
3. H.R. Oswald and W. Feitknecht, Helvetica Chimica Acta **47**, 272 (1964)
4. H.R. Oswald et al., Helvetica Chimica Acta **44**, 2103 (1941).
5. S. Miyahara and K. Ueda, Phys. Rev. Lett. **82**, 3701 (1999).
6. H. Kageyama et al., Phys. Rev. Lett. **84**, 5876 (2000).
7. R.W. Smith and D.A. Keszler, J. Solid State Chem. **93**, 430 (1991).
8. S. Miyahara and K. Ueda, cond-mat/0004260
9. C. Knetter et al., Phys. Rev. Lett. **85**, 3958 (2000).
10. A. Koga, J. Phys. Soc. Jpn. **69**, 3509 (2000).
11. M.P. Gelfand, Phys. Rev. B **43**, 8644 (1991).
12. K. Ueda and S. Miyahara, J. Phys.:Condens. Matter **11**, L175 (1999).
13. O. Cépas et al., Phys. Rev. Lett. **87**, 167205 (2001).
14. P. Lemmens et al., Phys. Rev. Lett. (2000).
15. K. Sparta et al., Eur. Phys. J. B **19**, 507 (2001).
16. H. Kageyama et al., Suppl. Prog. Theor. Phys., in press.
17. Z. Hiroi et. al., J. Phys. Soc. Jpn. **70**, 3377 (2001).
18. D. J. Hodgson, Prog. Inorg. Chem. **19**, 173 (1975).
19. J.N. Reimers and A.J. Berlinsky, Phys. Rev. B **48**, 9539 (1993).
20. J.T. Chalker et al., Phys. Rev. Lett. **68**, 855 (1992).
21. C. Zeng and V. Elser, Phys. Rev. B **42**, 8436 (1990).
22. C. Waldtmann et al., Eur. Phys. J. B **2**, 501 (1998).
23. C. Lhuillier and P. Sindzingre, proceedings of French-Japanese symposium, Hakata, Nov. 19-22, 2001, Fukuoka, Japan)
24. M. Elhajal et al., cond-mat 0108003; C.Lacroix, this conference.
25. T. Inami, Phys. Rev. B **61**, 12181 (2000).
26. T. Inami, Phys. Rev. B **64**, 054421 (2001).